ENHANCING THE AMPACITY OF A 400 KV OVERHEAD TRANSMISSION LINE UNDER REAL WEATHER CONDITIONS: A CASE STUDY USING THE CIGRE 601 METHODOLOGY

František MARGITA*, Ľubomír BEŇA*, Paweł PIJARSKI**, Sylwester ADAMEK**, Krzysztof BARAN***, Ardian HYSENI*, Kristián GLAJC*
*Department of Electric Power Engineering, Faculty of Electrical Engineering and Informatics, Technical University of Košice, Mäsiarska 74, 042 00 Košice, Slovak Republic,
E-mails: frantisek.margita@tuke.sk, lubomir.bena@tuke.sk, ardian.hyseni@tuke.sk, kristian.glajc@tuke.sk;
**Department of Power Engineering, Faculty of Electrical Engineering and Computer Science, Lublin University of Technology, Nadbystrzycka 38D, 20-618 Lublin, Poland,
E-mails: p.pijarski@pollub.pl, s.adamek@pollub.pl;
***Department of Power Electronics and Power Engineering, Faculty of Electrical and Computer Engineering, Rzeszów University of Technology, Al. Powstańców Warszawy 12, 35-959 Rzeszów, Poland,
E-mail: kbaran@prz.edu.pl.

ABSTRACT

A steady-state dynamic line rating (DLR) assessment was conducted for a 400 kV overhead transmission line in Slovakia using the standardized CIGRE Technical Brochure 601 methodology. The study was performed on the V427 corridor equipped with aluminium conductor steel-reinforced (ACSR) 243-AL1/39-ST1A conductors to evaluate the ampacity potential under realistic environmental conditions. Hourly meteorological data for the year 2024 were obtained from the Open Meteo API and included ambient temperature, wind speed and direction, and global tilted irradiance. The ampacity model accounted for Joule heating, solar gain, convective and radiative cooling, and the current limits were derived from the thermal equilibrium condition. The results showed that the average DLR exceeded the conventional static line rating (SLR) by 69.3 %, with exceedance observed during 99.4 % of the evaluated hours. The influence of weather parameters, particularly wind speed and angle of attack, on conductor performance was also quantified. These findings confirmed the feasibility of implementing DLR to enhance grid utilization, especially under conservative operating assumptions.

Keywords: *Dynamic Line Rating, Ampacity, Overhead Transmission Line, CIGRE 601, ACSR Conductor, Weather-based Modeling*

1. INTRODUCTION

The increasing integration of renewable energy sources and the growing complexity of power system operations imposed new requirements on the reliable and efficient utilization of transmission infrastructure. In this context, overhead line ampacity was recognized as a key operational constraint that directly affected system security, congestion management, and market efficiency [1].

Conventional SLR practices relied on conservative assumptions about ambient temperature, wind, and solar conditions. These static limits often underestimated the real-time current-carrying capacity of conductors, particularly under favorable weather. As a result, valuable transmission potential remained unutilized, limiting the integration of renewable generation and increasing redispatch costs [2].

DLR offered a promising alternative by continuously adjusting ampacity based on actual environmental conditions. International guidelines such as IEEE 738 [3] and CIGRÉ Technical Brochure 601 [4] provided well-established models for steady-state ampacity evaluation. However, their implementation was still associated with practical challenges, such as accurate weather characterization, proper model calibration, and regional validation under real-world conditions [5].

Furthermore, many implementations relied on real-time monitoring or forecast-based methods, while fewer studies addressed the use of high-resolution historical datasets for long-term planning and feasibility assessments [6].

To address these limitations, this paper presented a comprehensive steady-state DLR evaluation of a 400 kV transmission line in Slovakia using the standardized CIGRÉ 601 methodology. The model incorporated realistic conductor parameters and hourly meteorological data obtained from the Open-Meteo API [7]. A single reference point with conservative weather characteristics was used to ensure robustness under adverse operating conditions.

The main contributions of this paper are summarized below:

– *Region-specific implementation:* A regionally customized application of the CIGRÉ 601 ampacity model was developed for the 400 kV transmission line V427 in Slovakia, using the ACSR 243-AL1/39-ST1A conductor.

– *Data integration:* Open-access, high-resolution meteorological data were incorporated to generate hourly DLR profiles for an entire calendar year.

– *DLR vs. SLR quantification:* A statistical and seasonal comparison of dynamic and static line ratings was performed, identifying time periods with potential for operational enhancement.

– *Sensitivity analysis:* A detailed examination of the influence of wind speed, wind angle of attack, solar radiation, and ambient temperature on ampacity was carried out.

The rest of the paper is organized as follows: Section 2 introduces the test site and the meteorological dataset used in the study. Section 3 describes the calculation model and ampacity formulation according to CIGRÉ 601. Section 4 presents the numerical results, including annual and monthly ampacity profiles. Section 5 discusses the key findings and their implications. Section 6 concludes the paper and outlines directions for future work.

2. TEST SITE AND METEOROLOGICAL DATASET

2.1. Line overview

The 400 kV transmission corridor V427, operated by the Slovak transmission system operator SEPS, interconnects the substations in Rimavská Sobota and Moldava.

This line was selected as a case study for ampacity assessment under typical Central European climatic conditions (see Fig. 1). The surrounding terrain is moderately undulating, with an average elevation of approximately 210 m a.s.l [8].

2.2. Conductor specification

The ampacity calculation was carried out for the overhead transmission line V427 (Rimavská Sobota – Moldava), which was equipped with a standard ACSR cable of type 243-AL1/39-ST1A, manufactured in accordance with STN EN 50182. The conductor consisted of 26 aluminium strands and 7 steel strands, with respective diameters of 3.45 mm and 2.68 mm [9].

The mechanical and electrical parameters applied in the model were summarized in Table 1 [9].

The conductor core was assumed to be ungreased. Emissivity and absorptivity of the conductor surface were both assigned a value of $\varepsilon = 0.5$ and $\alpha = 0.5$, respectively, to represent aged bare conductors [9].

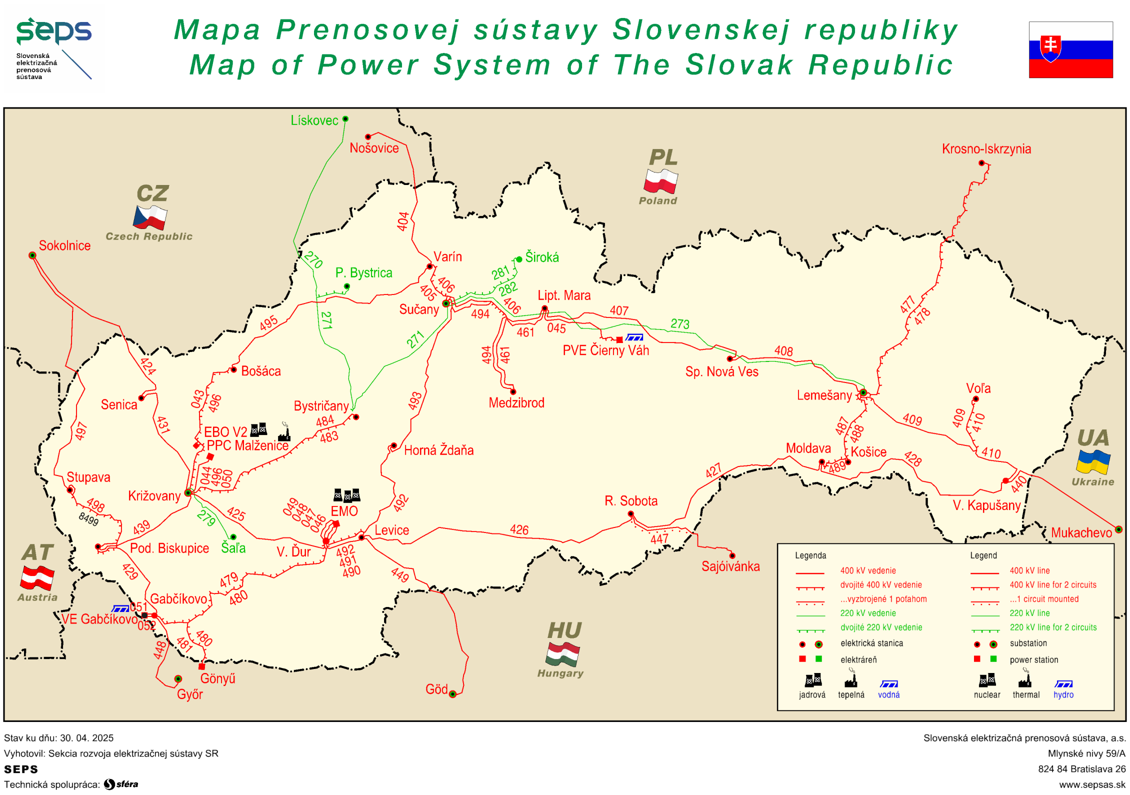

Fig. 1 Map of the transmission system of the Slovak Republic

3. CALCULATION MODEL

3.1. Weather data source

Meteorological data essential for the DLR calculations were retrieved from the Open-Meteo historical forecast API, which provides publicly available, high-resolution weather datasets. For the purposes of this study, the API was queried to obtain complete hourly weather profiles for the full calendar year 2024, using a single reference location situated in a southern valley near Rimavská Sobota [7].

Although the dynamic line rating analysis was performed along the entire 400 kV V427 transmission corridor (Rimavská Sobota–Moldava nad Bodvou), the Rimavská Sobota electrical substation was selected as the reference point for further evaluation due to its central position and simplicity of graphical representation.

A detailed assessment of the annual meteorological dataset revealed that the five least-favourable weather points (based on the year-long hourly data) were all located in the vicinity of the corridor section oriented towards the Rimavská Sobota substation (Table 2). For simplicity and representativeness of the annual thermal behaviour, this location was therefore adopted as the reference for the steady-state and dynamic ampacity evaluation. Although this specific point was not representative of spatially distributed conditions along the entire V427 transmission corridor Rimavská Sobota–Moldava), it was deliberately selected due to its conservative meteorological characteristics, including higher solar radiation and lower wind speeds. As a result, this location provided a lower-bound estimate of ampacity under unfavourable conditions [10].

Table 1 Mechanical and electrical parameters of ACSR 243-AL1/39-ST1A conductor [9]

Parameter	**Value**
Total cross-sectional area	282.54 mm^2
Aluminium cross-sectional area	243.05 mm^2
Steel cross-sectional area	39.49 mm^2
Number of aluminium strands	26
Number of steel strands	7
Aluminium strand diameter	3.45 mm
Steel strand diameter	2.68 mm
Overall conductor diameter	21.84 mm
Steel core diameter	8.04 mm
Conductor mass	980.1 kg km^{-1}
Rated tensile strength	85.12 kN
DC resistance at 20 °C	0.1188 $\Omega\,\text{km}^{-1}$
Modulus of elasticity	73 867 N mm^{-2}
Linear thermal expansion coefficient	$18.87 \times 10^{-6}\,\text{K}^{-1}$

The dataset comprised the following key atmospheric variables: ambient air temperature at 2 meters above ground level (°C), as illustrated in Fig. 2; wind speed at 10 meters above ground level (m/s), as shown in Fig. 3; wind direction at 10 meters above ground level (° from north, meteorological convention), from which the wind angle of attack was subsequently derived (Fig. 4); and global tilted irradiance (W/m^2), denoting the total shortwave solar radiation incident on an optimally tilted surface. This quantity corresponded to the global tilted irradiance affecting the conductor surface under real-world operating conditions and is depicted in Fig. 5.

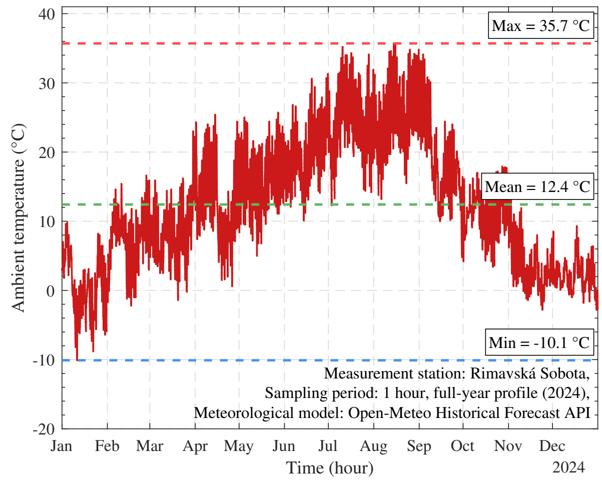

Fig. 2 Ambient temperature profile from the Rimavská Sobota power station over a period of one year

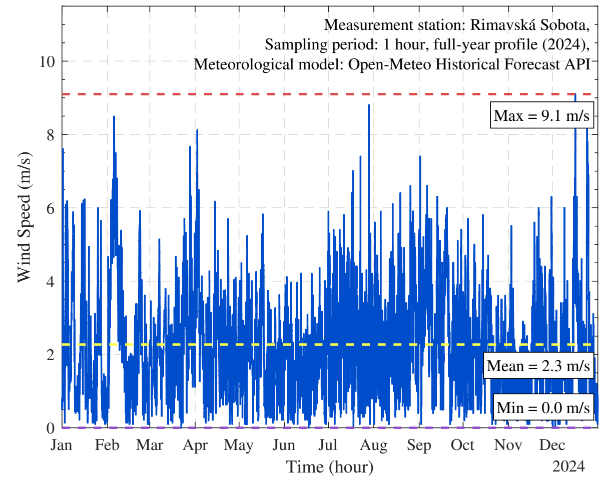

Fig. 3 Annual wind speed profile measured at the Rimavská Sobota power station

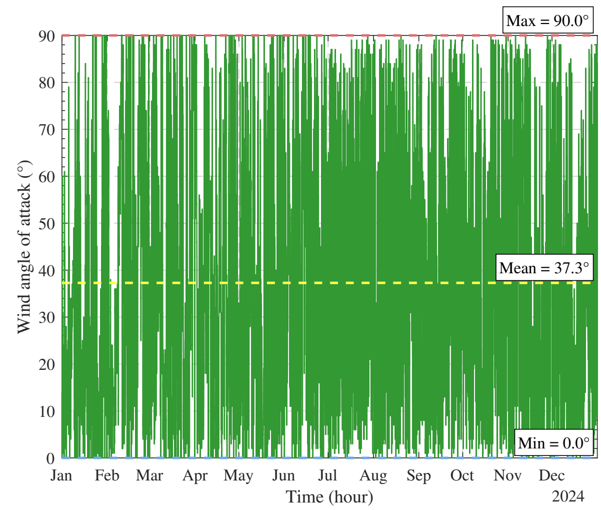

Fig. 4 Annual profile of the wind angle of attack at the Rimavská Sobota power station

Table 2 Top-5 least-favourable points along the V427 corridor based on the annual mean weather conditions (2024)

Latitude [°]	Longitude [°]	Ambient temperature [°C]	Wind speed [m/s]	Solar radiation [W/m^2]	Wind attack angle [°]
48.391	20.333	11.81	7.44	154.17	37.60
48.356	20.291	11.75	7.33	155.25	39.90
48.351	20.199	11.67	7.46	155.41	49.11
48.324	20.253	11.67	7.46	155.41	49.11
48.427	20.374	10.95	7.44	154.17	37.60

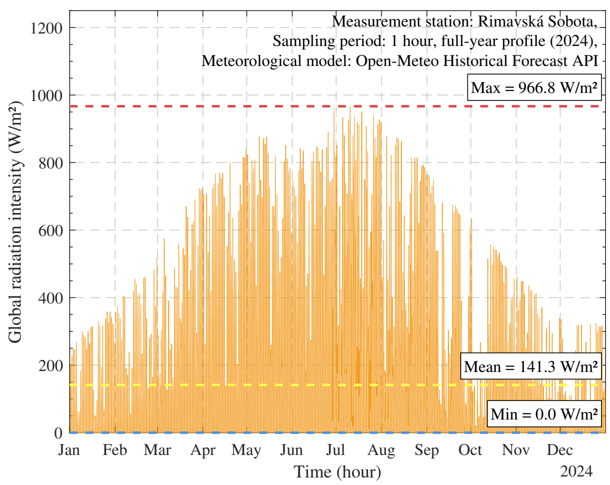

Fig. 5 Temporal distribution of global tilted irradiance at the Rimavská Sobota site throughout the year

These parameters served as critical inputs to the thermal balance equations employed for ampacity evaluation, in accordance with the methodology described in [4].

An additional derived variable, the wind angle of attack, was computed for each hourly interval based on the known azimuthal orientation of the overhead line (fixed at 90° eastward) and the instantaneous meteorological wind direction. The angle of attack determined the effective component of wind velocity perpendicular to the conductor axis, which directly influenced the convective heat transfer coefficient. For the purposes of thermal modeling, this angle was symmetrized to the range $[0°, 90°]$ by assuming aerodynamic symmetry of the conductor cross-section [4].

4. STEADY-STATE DYNAMIC LINE RATING ACCORDING TO CIGRE 601

4.1. Steady state heat balance

The thermal state of overhead conductors was influenced by ambient temperature, wind speed and direction, solar radiation, and the electric current. When these parameters remained approximately constant, the system reached a steady-state condition, in which both the conductor temperature and the current stabilized. In this regime, heat gains resulting from Joule losses and solar radiation were balanced by convective and radiative cooling. Additional effects, such as corona losses, magnetic core losses, or evaporative cooling, could also be taken into account.

The steady-state condition was described by the heat balance equation [4]:

$$P_\mathrm{J} + P_\mathrm{S} + P_\mathrm{M} + P_\mathrm{i} = P_\mathrm{c} + P_\mathrm{r} + P_\mathrm{w}, \tag{1}$$

where P_J, P_S, P_M, P_i, P_c, P_r and P_w denote, respectively, Joule heating, solar heat gain, magnetic core heating, corona heating, convective cooling, radiative cooling, and evaporative cooling per unit length (W·m^{-1}).

Under specific environmental conditions, such as high humidity combined with strong wind, corona heating could have contributed to the overall thermal input. Nevertheless, its effect was typically neglected in ampacity calculations, as convective cooling under such conditions tended to dominate. Likewise, although evaporative cooling could have influenced the conductor temperature, it was generally excluded from thermal models due to its rare occurrence and the difficulty of accurate quantification. For conservative steady-state thermal assessments, both effects were omitted, and the simplified heat balance was expressed as [4]:

$$P_\mathrm{J} + P_\mathrm{S} + P_\mathrm{M} = P_\mathrm{c} + P_\mathrm{r} \tag{2}$$

Furthermore, the magnetic heating term P_M was often accounted for by incorporating it into the Joule heating through an increased effective conductor resistance. This approach resulted in a more general and practically used expression [4]:

$$P_\mathrm{J} + P_\mathrm{S} = P_\mathrm{c} + P_\mathrm{r} \tag{3}$$

4.2. Steady state thermal rating

A numerical procedure for evaluating the steady-state thermal rating of an overhead conductor under fixed (expected) weather conditions and a prescribed maximum allowable conductor temperature $T_{\mathrm{c,max}}$ was illustrated in Fig. 6.

Under fixed weather conditions, namely wind speed, wind direction, ambient temperature, and solar irradiance, the first step consisted in evaluating the convective cooling power P_c, the radiative cooling power P_r, and the AC resistance of the conductor R_ac at the given conductor temperature T_c.

The permissible current I was then determined by rearranging the steady-state heat balance equation (3) as [4]:

$$I = \sqrt{\frac{P_c(T_c) + P_r(T_c) - P_S}{R_{ac}(T_c)}} \tag{4}$$

In order to apply the procedure, a set of physical and meteorological inputs was required. The reference DC resistance at 20 °C (R_{DC20}) together with the linear temperature coefficient of resistance (α) defined the temperature dependence of conductor resistance, which entered the Joule heating term. The overall conductor diameter (D) specified the external surface per unit length and was necessary for the evaluation of the Reynolds number and heat exchange, whereas the strand diameter (d) was used to estimate the AC resistance through skin and magnetisation effects. The kinematic viscosity of air (ν), wind speed (V), and wind attack angle (δ) governed the convective heat transfer coefficient according to the Morgan correlations. The ambient air temperature (T_a) set the gradient for both convection and radiation, while the global tilted irradiance (I_T) represented the external heating source. The surface emissivity (ε_s) determined the radiative cooling power, and the absorptivity (α_s) defined the absorbed fraction of incident solar radiation. Finally, the conductor temperature (T_c) was the state variable obtained from the thermal balance, and its comparison with the admissible thermal limit established the steady-state ampacity.

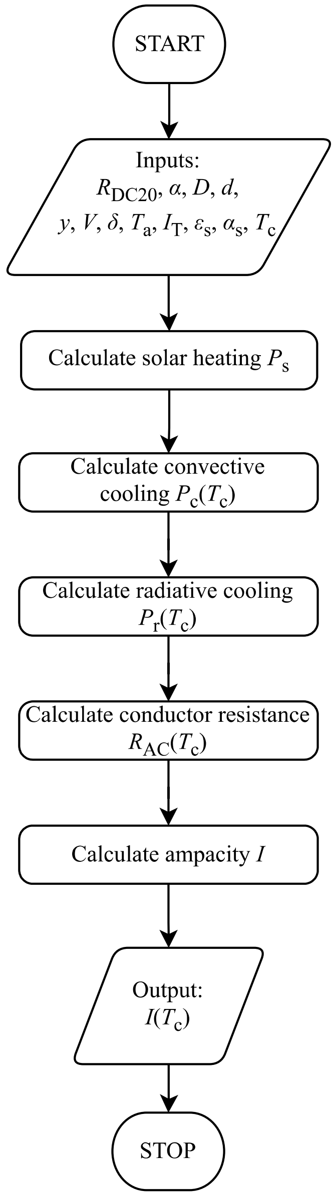

Fig. 6 Flowchart representing the calculation procedure for steady-state DLR

5. RESULTS

The steady-state DLR was evaluated for the 400 kV transmission line V427 connecting Rimavská Sobota and Moldava, based on hourly weather data for the year 2024. The computed DLR ranged from 460.4 A to 1731.6 A, with an annual mean of 926.0 A. In comparison to the SLR of 547 A, the average ampacity represented a 69.3 % increase.

Fig. 7 presents the hourly DLR values over the course of the year. The percentile distribution of the ampacity values is shown in Fig. 8, indicating that the DLR exceeded the SLR during 99.4 % of the year, corresponding to 8734 hours. Only 50 hours (0.6 %) fell below the static limit. The average ampacity gain during periods when DLR exceeded the SLR was 381.3 A.

To evaluate the seasonal influence of weather on the ampacity of the V427 overhead line, Table 3 presents the monthly averages of ambient air temperature, wind speed, solar radiation, wind angle of attack, and the resulting steady-state DLR values, based on hourly data from the year 2024.

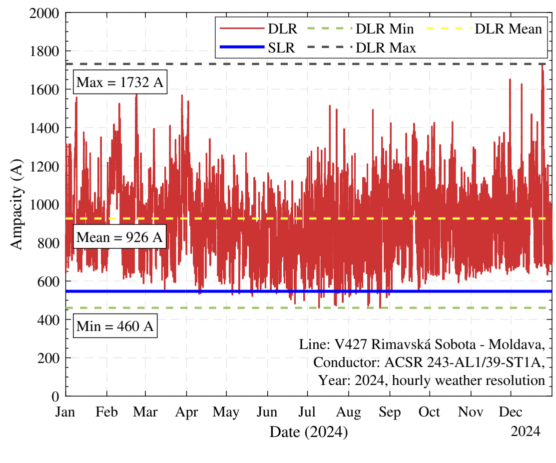

Fig. 7 Annual hourly profile of steady-state DLR and reference SLR for the V427 line during 2024

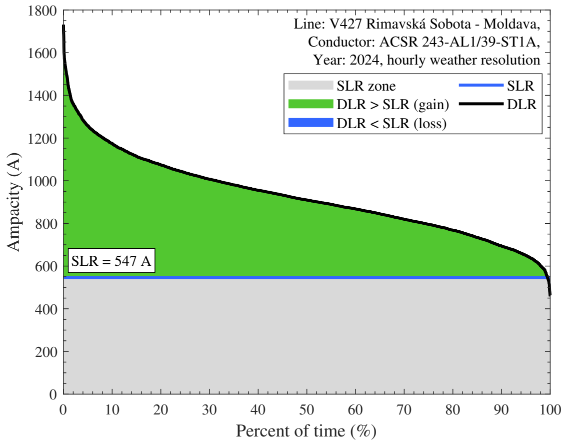

Fig. 8 Annual sorted profile of DLR vs. SLR for line V427 using 2024 hourly weather data (ACSR 243-AL1/39-ST1A)

The average ambient temperature increased from 0.25 °C in January to a peak of 25.34 °C in August. This rise in temperature was correlated with a gradual decrease in average ampacity, which dropped from 932 A in January to its minimum value of 831 A in June. This inverse relationship was consistent with the physical principle that higher conductor temperatures reduce current-carrying capacity due to increased electrical resistance.

Monthly average wind speeds remained relatively stable throughout the year, ranging from 1.82 m/s in June to 2.93 m/s in September. Notably, higher average wind speeds in February, March, and September coincided with increased ampacity, which could be attributed to enhanced convective heat transfer.

The average wind angle of attack varied moderately across the months, from 26.7 ° in January to 42.0 ° in July. As this angle determined the component of wind perpendicular to the conductor, it directly influenced the convective cooling efficiency.

Solar radiation followed a typical seasonal trend, with the highest monthly average values observed in May and June, both exceeding 250 W/m^2. Although increased solar gain contributed additional thermal load, its negative impact on ampacity was largely offset by favorable wind conditions and moderate wind incidence angles during these periods.

The maximum hourly DLR value was recorded in December (1732 A), most likely during a short interval of strong wind and low ambient temperature. In contrast, the lowest hourly ampacity occurred in July and August, when high air temperatures and limited convective cooling constrained the current-carrying capacity.

At the hour of the lowest ampacity (460.4 A; 2024-00-24 14:00), the ambient temperature was 32.4 °C, the wind speed was 0.5 m/s with a wind angle of attack of 63°, and the global tilted irradiance reached $I_T = 739$ W/m^2. Conversely, the maximum ampacity (1731.6 A; 2024-00-24 15:00) coincided with a cold and windy hour, with $T_a = 3.7$ °C, $v = 8.2$ m/s, $\delta = 47°$, and $I_T = 89$ W/m^2.

6. DISCUSSION

The analysis confirmed that the ampacity of overhead conductors exhibited significant variability driven by ambient weather conditions. An inverse correlation between temperature and ampacity was observed, with monthly average ampacity decreasing during the summer months despite elevated levels of solar radiation. Although solar irradiance increased the thermal input, its effect was often offset by convective cooling when wind speeds were sufficient. However, during periods of high temperature and low wind, the reduction in ampacity became pronounced.

The wind angle of attack also played a critical role in determining the effectiveness of convective cooling. Months with favorable wind incidence (i.e., a high perpendicular component relative to the conductor axis) exhibited elevated ampacity even at moderate wind speeds. This finding highlighted the importance of resolving not only wind magnitude but also wind direction when calculating the convective heat transfer coefficient.

7. CONCLUSION

Although the analysis was based on a single meteorological reference point located in the southern valley near Rimavská Sobota, rather than on a distributed set of measurements along the entire V427 transmission corridor, the results provided a robust foundation for assessing the steady-state DLR potential over the course of the year. The derived ampacity profiles confirmed that weather-dependent thermal behavior could be reliably estimated even from a localized dataset, provided it was representative of prevailing climatic conditions.

This approach was found to be suitable not only for routine operational enhancement through steady-state DLR application, but also for supporting transient thermal assessments in critical dispatch scenarios. These included load reallocation, outage planning, and congestion mitigation under short-term stress conditions.

Future research will focus on extending the methodology to incorporate spatially distributed meteorological inputs and real-time sensor integration to improve accuracy and enhance operational confidence.

Furthermore, future efforts will aim at developing a fully operational DLR software framework for both steady-state and transient evaluations. Particular attention will be given to the detailed assessment of ampacity in the context of existing infrastructure limitations of the Slovak transmission system operated by SEPS. Adaptation of DLR methodologies to medium and high voltage distribution lines, particularly at the 110 kV level, will also be investigated. Finally, the economic implications of DLR integration will be examined, including its impact on electricity market efficiency, redispatch costs, and renewable integration strategies.

In addition, it was recommended that future analyses should incorporate sub-hourly meteorological and solar input datasets, preferably with a temporal resolution of at least 15 minutes. This enhancement would allow for a more accurate representation of rapid variations in wind speed

Table 3 Monthly average weather conditions and steady-state DLR for the year 2024

Month	Temp. [°C]	Wind speed [m/s]	Wind angle [°]	Solar rad. [W/m²]	DLR avg. [A]	DLR min [A]	DLR max [A]
1	0.25	2.09	27	50	932	643	1557
2	7.21	2.70	40	74	1019	588	1590
3	8.28	2.32	39	126	973	558	1569
4	12.49	2.43	39	199	956	533	1537
5	16.15	1.94	34	251	855	522	1267
6	20.01	1.82	41	258	832	483	1163
7	24.27	2.39	42	239	874	461	1514
8	25.34	2.46	39	187	869	460	1492
9	18.65	2.93	40	126	976	553	1423
10	11.06	2.10	37	86	925	593	1429
11	3.22	1.94	37	63	939	617	1651
12	1.93	2.16	33	37	968	633	1732

and solar irradiance, which can cause significant short-term fluctuations in conductor temperature and ampacity. The temporal and spatial resolution of weather data was identified as a critical factor, since hourly observations from stations located farther from the transmission corridor and affected by distinct microclimatic conditions may introduce additional uncertainty into the ampacity estimation process.

ACKNOWLEDGEMENT

This paper was supported by the Science Grant Agency of the Ministry of Education, Research, Development and Youth of the Slovak Republic under the contract VEGA 1/0532/25.

REFERENCES

[1] MARGITA, F. – BEŇA, Ľ. – MAŁSKA, W. – PIJARSKI, P.: Possibilities of Increasing the Ampacity of Overhead Lines Using High-Temperature Low-Sag Conductors in the Electric Power System of the Slovak Republic. *Applied Sciences*, vol. 14, p. 7846, Sep. 2024. DOI: https://doi.org/10.3390/app14177846

[2] MARGITA, F. – BEŇA, Ľ. – PIJARSKI, P.: Calculation of the Ampacity of Overhead Power Lines Under the Conditions of the Electric Power System of the Slovak Republic. In: *Proceedings of the 24th International Scientific Conference on Electric Power Engineering (EPE)*, 2024, pp. 1–5. Available online: https://doi.org/10.1109/EPE61521.2024.10559565

[3] IEEE Power and Energy Society: *IEEE Standard for Calculating the Current–Temperature Relationship of Bare Overhead Conductors*, IEEE Std 738–2023 (Revision of IEEE Std 738–2012). Approved on June 29, 2023; Published on December 19, 2023. ISBN: 978–1–5044–9820–3 (PDF), 978–1–5044–9821–0 (Print).

[4] CIGRÉ Working Group B2.42: *Guide for Thermal Rating Calculations of Overhead Lines*. CIGRÉ Technical Brochure 601, 2014.

[5] MARGITA, F. – BEŇA, Ľ.: The Use of WAM Systems for Determining the Ampacity of Overhead Power Lines. *Acta Universitatis Sapientiae Electrical and Mechanical Engineering*, vol. 16, pp. 96–109, 2024. Available online: https://doi.org/10.47745/auseme-2024-0009. ISSN 2065-5916.

[6] MALSKA, W.: Analysis of Current Ampacity of the 110 kV Overhead Transmission Line Using a Multiple Regression Model. *Electric Power Systems Research*, vol. 236, p. 110939, 2024. ISSN: 0378–7796. Available online: https://doi.org/10.1016/j.epsr.2024.110939

[7] OPEN–METEO: Open–source weather API for non–commercial use. Available online: https://open-meteo.com/ (accessed on July 22, 2025)

[8] SLOVAK ELECTRICITY TRANSMISSION SYSTEM, INC. (SEPS): Grid schemes of the Slovak transmission network. *Official SEPS website – Technical parameters*, 2025. Available online: https://www.sepsas.sk/pre-partnerov/technicke-parametre/schemy-siete/ (accessed on July 15, 2025)

[9] STREDOSLOVENSKÁ ENERGETIKA, A.S.: Technical specification of ACSR 243-AL1/39-ST1A conductor. *Online cable database SSE*, 2023. Available online: https://online.sse.sk/pls/kpfc/kpfc_web.detail?meno=&idk=1&ids=3&csap=25257.02 (document ID: SAP 25257, approved on July 15, 2023)

[10] SZPYRA, W. – KACEJKO, P. – PIJARSKI, P. – WYDRA, M. – KMAK, J. – NOWAK, W. – TARKO, R.: Dynamic Management of Transmission Capacity in Power Systems. *Acta Energetica*, vol. 4, pp. 68–77, Jul. 2018. Available online: https://doi.org/10.12736/issn.2300-3022.2017406

Received September 21, 2025, accepted November 21, 2025

BIOGRAPHIES

František Margita received his Bachelor's degree in Intelligent Systems from the Department of Cybernetics and Artificial Intelligence at the TUKE in 2021. He then completed his Engineer's degree in Electrical Power Engineering at the Department of Electric Power Engineering at TUKE in 2023, with a diploma thesis focused on the use of WAM systems to determine the ampacity of overhead transmission lines. Since 2023, he has been pursuing a PhD at the same department, specializing in Industrial Electrical Engineering. His doctoral research focuses on the topic of dynamic line rating of overhead transmission lines under Slovak climatic conditions. His research interests include dynamic ampacity assessment of overhead transmission lines, modeling based on meteorological data, application of CIGRE and IEEE standards, optimization of transmission capacity, and integration of DLR into power system operation and control. He is proficient in MATLAB, Python, SQL, R, and advanced data analytics applied to energy systems.

Ľubomír Beňa received his MSc degree in 1998 from the Department of Electric Power Engineering, Faculty of Electrical Engineering and Informatics, Technical University of Košice (TUKE). He earned his PhD in 2001, specializing in the mechanics of overhead power lines. Since 2010, he has served as an Associate Professor at the Department of Electric Power Engineering at TUKE. His scientific, professional, and teaching activities focus on the analysis and optimization of power system operation, the impact of renewable energy sources (RES) on distribution grids, and the study of the mechanical properties of overhead lines.

Paweł Pijarski, associate professor, is a graduate of the Faculty of Electrical Engineering and Computer Science at the Lublin University of Technology in Poland. He completed his master's degree in 2004. In 2012, he obtained the academic degree of doctor (PhD). In 2019, he obtained the academic degree of doctor habilitated (DSc, habilitation). Since 2005, he has been working at the Department of Power Engineering at the Faculty of Electrical Engineering and Computer Science at the Lublin University of Technology. His scientific interests are related to the analysis and assessment of the operating conditions of the power system, as well as metaheuristic optimization methods.

Sylwester Adamek graduated from the Faculty of Electrical Engineering at the Lublin University of Technology, specializing in electrical power engineering. In 2001, he began working as an assistant. In 2010, he earned a doctorate in technical sciences from the Faculty of Electrical Engineering and Computer Science at the Lublin University of Technology. His scientific interests include power system operation, power generation, and power engineering operations and measurements.

Krzysztof Baran graduated with a MSc degree from the Faculty of Electrical Engineering and Computer Science at the Rzeszów University of Technology in 2011. In 2019, he earned his doctorate and has been working as an Assistant Professor in the Department of Power Electronics and Electrical Power Engineering since that year. His research activities include lighting technology, thermal analysis of high-power LEDs, as well as thematic areas related to electrical power engineering and renewable energy sources.

Ardian Hyseni is a PhD student at the Department of Electrical Power Engineering, Technical University of Košice. He received his Bachelor's degree in 2020 with a thesis focused on the Design of a Teaching Aid for Power Engineering, and his Master's degree (Ing.) in 2023 with a thesis titled Benford's Law and Its Application in Power Engineering. His current research focuses on the analysis of big data in electrical distribution networks, aimed at increasing the reliability and efficiency of power distribution.

Kristián Glajc in 2023 he graduated (Ing.) in the field of power engineering at the Faculty of Electrical Engineering and Informatics, Technical University of Košice. Since 2024 he has been a PhD student at the Department of Electrical Power Engineering. His research focuses on the investigation of electrical discharges in nanofunctionalized transformer oil and on diagnostic methods including electrical, optical, and acoustic techniques. His work further includes the evaluation of nanofluid stability, the behaviour of nanoparticles in transformer oils, and their impact on the long-term reliability of liquid insulation in high-voltage systems.